ENGINEERING TRANSACTIONS • Engng. Trans. • 51, 4, 399–418, 2003
Polish Academy of Sciences • Institute of Fundamental Technological Research
10.24423/engtrans.479.2003

DYNAMIC CHARACTERISTICS OF AN EXPERIMENTAL MR FLUID DAMPER

B. Sapiński

Department of Process Control,
AGH - University of Science and Technology
al. Mickiewicza 30, 30-059 Kraków
e-mail:deep@uci.agh.edu.pl

The paper provides the results of experimental studies of dynamic characteristics of a linear MRF damper, designed specially for research purposes. Two MR fluids having different viscosity were used in the experiments. Damper design and parameters of the applied MR fluids are discussed. The relationship between the damping force and piston velocity was determined and utilised to identify the involution model of the damper. Currents in the coil were measured for voltage excitations with pulse width modulation and parameters of equivalent model of the control system were identified.

Key words: MR fluid, MRF damper, dynamic characteristics, analytical model, control system, identification.

1. Introduction

Rapid advancements in material engineering led to the invention of new materials, known as "smart". As these materials have become commercially available, the areas of their applications extend rapidly. This group of materials includes electrorheological fluids (ERF) and magnetorheological fluids (MRF), which are already applied in machine engineering and the construction industry [5]. An example of such applications are controlled mechanical vibration dampers allowing for modification of structural vibrations. The distinguishing feature of ER and MR fluids is that their viscosity changes by several orders of magnitude in the presence of electric or magnetic field [1]. The applications of MR fluids are now more widespread. New dampers in which damping characteristics change continuously have been designed and fabricated [3, 4, 10, 11, 12]. These dampers act as interfaces between electronic control systems and mechanical systems. Their structure is rather simple, the number of mobile components is small and they work fast and noiselessly. New commercially available devices were fabricated, in which the unique features of MR fluids are made use of; these include: a MagneRide shock absorber manufactured by Automotive Delphi Systems, a damper for the driver's seat RD-1005 manufactured by Lord Corporation, a suspension for the Cadillac car.

Dynamic characteristics of MRF dampers are strongly non-linear, which appears to be their inherent feature. These non-linearities are mostly a result of non-linearity introduced by the magnetic circuit consisting of ferromagnetic elements of the damper and the portion of MR fluid affected by the magnetic field excited by the current flowing through the coil(s) [6]. Hence the processes in MR fluids and the properties of coil circuit would determine the dynamic behaviour of the damper. The time constants (the electric constant and the coefficient of viscosity change) were determined as a part of the investigations of response time of linear MR dampers. These coefficients are considered in the simplified model of damper dynamics providing the relationship between the damping force and piston velocity. The values of these time constants are as follows: the electric time constant: from 1 ms to 200 ms; the time constant of viscosity variation ranges from 1 ms to 10 ms.

The results presented in this paper were obtained for an experimental linear MRF damper with a ring-shaped gap, designed and fabricated by the author as a part of his research program. The other device, i.e. a damper with a contactless piston sealing [10] is being investigated right now and the results will be published soon.

The main objectives of the tests were as follows:

- to find damper characteristics for two types of MR fluids, while the intensity of the control current is varied too,
- to identify the parameters in the involution model of the damper,
- to determine the coil current for voltage excitations with pulse width modulation,
- to identify the parameters of the equivalent model and control system of the damper.

In the first stage, the damper characteristics were investigated throughout the full range of control currents, i.e. from 0.0 A to 1.4 A. In the second stage the characteristics were obtained for the range 0.0 A to 0.20 A, which is the effective current for further control purposes. This range corresponds to those states of the damper when the shear stress is linearly related to shear strain of the MR fluid.

2. STRUCTURE OF AN EXPERIMENTAL DAMPER

Structure of an experimental MRF damper and its major components is shown in Fig. 1. The design of the damper is based on general principles of MRF dampers provided in [2], it is presented in more detail in [9]. The main design considerations are: the maximal axial force loading 3000 N; the maximal frequency of loading cycle variation – 10 Hz, admissible working temperature 360 K, damper size – the maximal length when the piston rod is maximally protruded – 260 mm, the largest admissible diameter 55 mm. This structure has several advantages: the damper is easily filled with working fluids in laboratory conditions and is easy to assemble and disassemble.

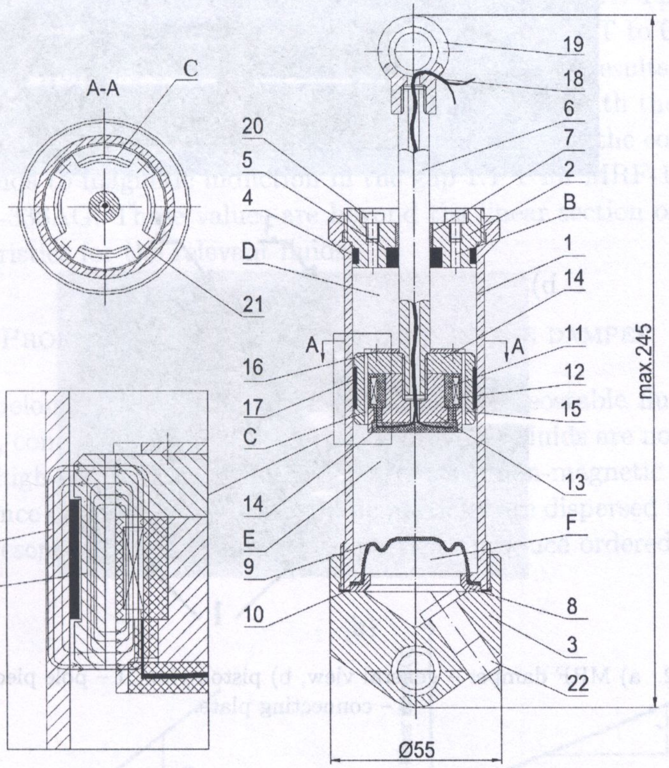

FIG. 1. Damper structure: 1 – housing, 2 – piston rod-end cover, 3 – free end cover, 4 – cover seal, 5 – piston rod sealing, 6 – piston rod, 7 – guiding element, 8 – pressing ring, 9 – diaphragm, 10 – ring-shaped sealing element, 11 – coil electric insulation, 12 – control coil, 13, 14 – pole pieces, 15 – outer flange of the piston, 16 – connecting plate, 17 – outer flange sealing, 18 – coil supply lead, 19 – piston rod holder, 20 – threaded corks; 21 – tap screws; 22 – dosing and cutting-off valve; B – opening for MR fluid dosing; C – ring-shaped gap for MR fluid flow; D – space inside the damper on the piston rod side; E – space inside the damper on the membrane side; F – space inside the damper under the membrane, M_g – main magnetic circuit (closed by the outer flange of the piston), M_p – ancillary magnetic circuit (closed with the housing).

The experimental MRF damper is shown in Fig. 2a. There is a one-sided piston rod and a ring-shaped gap which allows the fluid to flow between the piston and the cylindrical housing. The MR fluid filling the damper flows through that gap from one cavity to the other, depending on the direction of piston motion. One element of the piston assembly is a control coil. Current flowing through that coil excites the magnetic field. The coil is supplied through the lead whose ends are let out of the damper via an axial hole in the piston rod.

a)

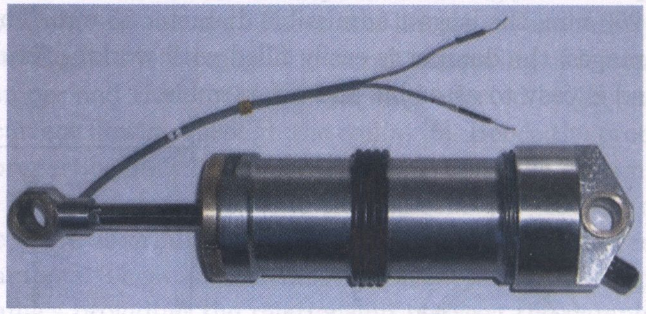

b)

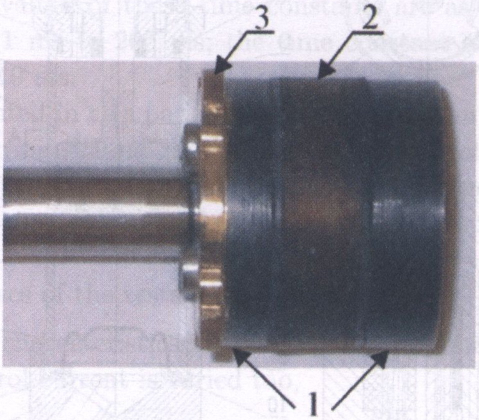

FIG. 2. a) MRF damper – general view, b) piston view: 1 – pole pieces, 2 – coil, 3 – connecting plate.

To allow for smooth damper operation, the magnetic field should not extend beyond the pole pieces width, no matter what is the piston position. In order to achieve that, damper elements should be made from materials displaying specified magnetic properties. The external part of the piston assembly (pole pieces, outer flange) and cylindrical housing are made of ferromagnetic materials while the remaining damper components (including the connecting plate) are made of diamagnetic materials. Owing to the careful selection of materials, the magnetic field generated in the coil passes through the MR fluid in the ring-shaped gap and is therefore closed with the damper housing over the length limited by the piston height. It is worthwhile to notice (see Fig. 1) that there are two magnetic circuits: the main circuits (M_g) closed by the outer flange and the ancillary one (M_p) closed by the housing. The main circuit controls the variations of damping characteristics (as the result of MR fluid viscosity changes) while the main task of the ancillary circuit is to ensure effective piston sealing.

The coil in the damper presented here is toroidal-shaped (Fig. 2b). For the purpose of experiments, the coils have different parameters determined on the basis of magnetic field distribution in the gap [8]. The type of supplying lead, its cross-section and the number of coil windings were such that magnetic induction in the gap would always fall in the linear section of magnetisation characteristics of the applied MR fluids for the control current range (0.0, 0.2) A. This interval corresponds to magnetic induction in the gap ranging from 0.0 T to 0.27 T (for MRF-132LD) and from 0.0 T to 0.20 T for MRF-336 AG. The results presented here were obtained for one of the coils, made of copper cable with the diameter 28 mm, having 215 windings. The maximal current intensity in the coil is 1.4 A, which corresponds to magnetic induction in the gap 1.1 T for MRF-132LD and 0.9 T for MRF-336AG. These values are beyond the linear section of magnetisation characteristics for the relevant fluids.

3. Properties of MR fluids used in the damper

MR fluids belong to the group of non-Newtonian, rheostable fluids having the yield stress, controllable by the magnetic field. These fluids are non-colloidal suspensions of high-concentration magnetic particles in non-magnetic carrier fluids. In the absence of magnetic field, magnetic particles are dispersed in a carrier fluid. In the presence of magnetic field the particles produce ordered chain-like structures [1].

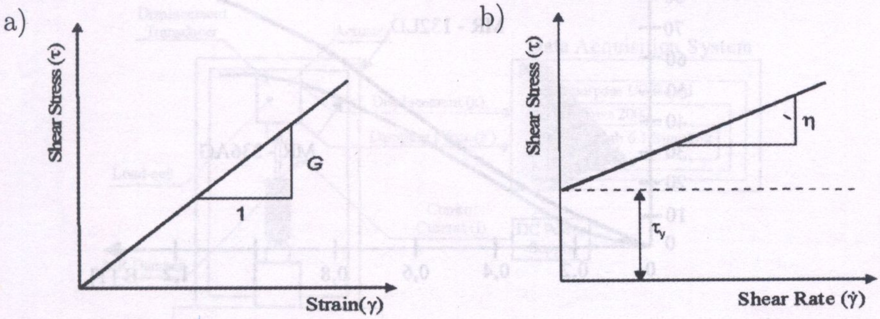

FIG. 3. The behaviour of magnetorheological fluids:
a) in pre-yield region: $\tau = G^*\gamma$, $\tau < \tau_y(H)$;
b) the behaviour of magnetorheological fluids in post-yield region:
$\tau = \tau_y(H) + \eta\dot{\gamma}$, $\tau \geq \tau_y(H)$.

In Fig. 3 G^* is complex shear modulus related to magnetic field strength H, η – plastic viscosity, γ – strain, $\dot{\gamma}$ – shear rate.

Rheological properties of MR fluids depend on the solid (magnetic particles) concentration, particles' size and shape, rheological properties of carrier fluids, presence of surfactants and admixture of substances improving lubrication, as well as external factors, particularly the magnetic field strength.

Magnetorheological fluids used in the tested damper are: MRF-132LD and MRF-336AG manufactured by Lord Corporation; these fluids are specially intended for vibration dampers. Main parameters of these MR fluids are compiled in Table 1 while the magnetisation characteristics and rheological characteristics are given in Fig. 4a and Fig. 4b.

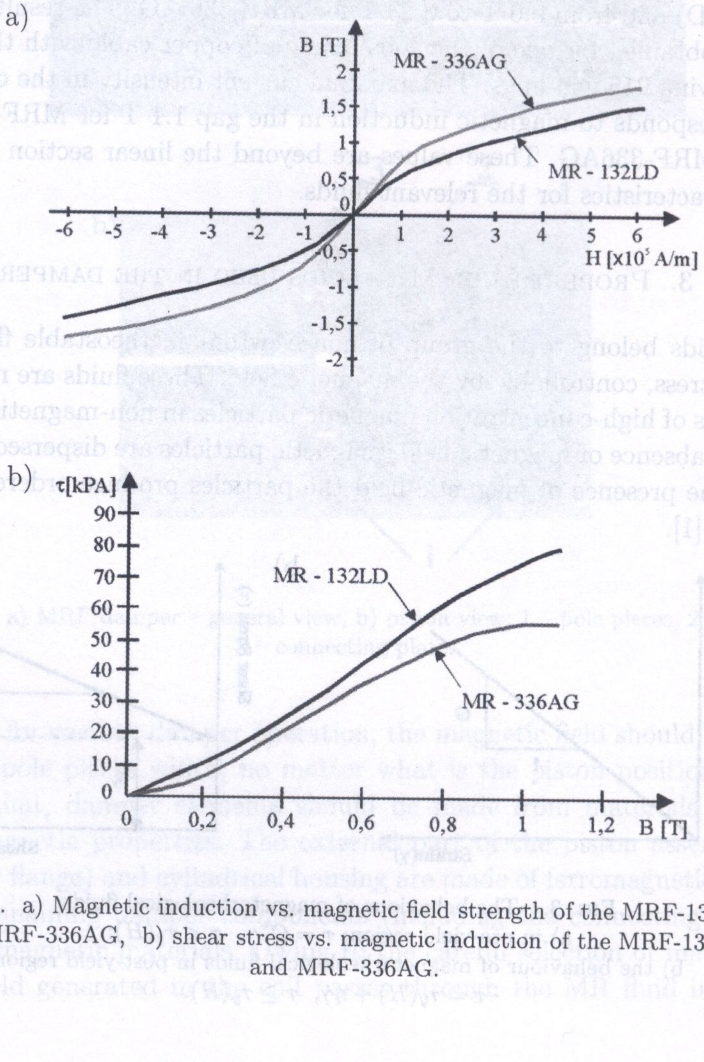

FIG. 4. a) Magnetic induction vs. magnetic field strength of the MRF-132LD and MRF-336AG, b) shear stress vs. magnetic induction of the MRF-132LD and MRF-336AG.

Table 1. Parameters of the MRF-132LD and the MRF-336AG.

Parameters	MRF-132LD	MRF-336AG
Carrier fluid	synthetic oil	silicone
Particles [µm]	iron ~3	iron ~3
Concentration by volumne ϕ [%]	32	36
Concentration by weight φ [%]	80.74	82.02
Viscosity [Pa·s] *)	0.94 (at 10 s^{-1}) 0.33 (at 80 s^{-1})	8.5 (at 10 s^{-1}) 4.4 (at 80 s^{-1})
Density ρ [g/cm^3]	3.055	3.446
$\eta/\tau_y^2(H)$ [s/Pa] **)	$6{\cdot}10^{-11}$	$2{\cdot}10^{-10}$
Saturation of particles J_s [T]	2.1	2.1
Operating temperature	– 40°C to +150°C	– 40°C to +150°C
Time response***)	miliseconds	miliseconds
Applications	multi-purposes, dampers, brakes, mount	mounts, dampers

*) – viscosity is a function of shear rate, **) – the parameter representing ratio of viscosity and max. shear stress squared, ***) – exact time response is dependent on a device.

4. Experiments at vibration – testing machine

The damper was examined in the experimental setup, (Fig. 5), with a computer-controlled vibration testing machine (Instron). Input-output data was acquired by using data acquisition system which was based on PC (Pentium III/1GHz) and multipurpose I/O board (RT-DAC4), operating in the software environment of Windows 2000, MATLAB/Simulink and Real Time Windows Target [13].

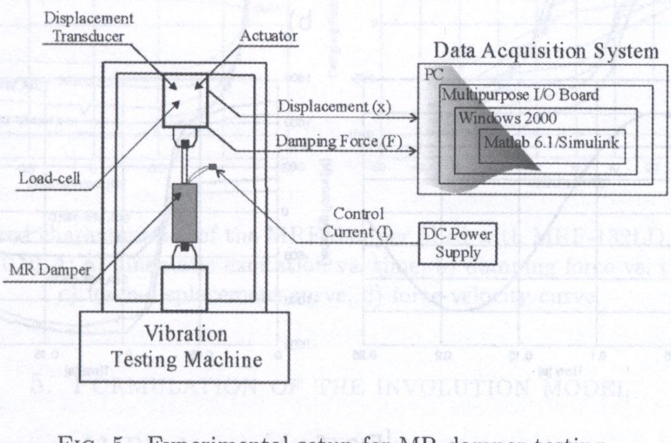

FIG. 5. Experimental setup for MR damper testing.

In first stage of experiments, the machine was programmed to generate a sinusoidal wave for three levels of frequency (1, 2.5, 4) Hz which correspond to the following values of amplitude $(10, 4, 1.5)\times10^{-3}$ m. The responses were measured for following levels of the applied current as follows: (0.0, 0.1, 0.2, 0.3, 0.4, 0.5, 0.6, 0.7, 0.8, 1.0, 1.2, 1.4) A. In the second stage, the frequency was (1; 2.5; 5) Hz and amplitude $(10; 4, 1.2)\times10^{-3}$ m, respectively. The responses were measured for five levels of the applied current, (0.0; 0.05, 0.10, 0.15, 0.20) A. Then the time history of piston velocity was computed. This data allowed us to determine dynamic characteristics of the damper (Fig. 6 and Fig. 7). Figure 6 presents with the damper filled with the MRF-132LD and the MRF-336AG respectively, by kinematic excitation (frequency 4 Hz, amplitude 1.5×10^{-3} m) and applied current of 0.0 A and 0.4 A. Although the measured characteristics of the damper filled with both types of MR fluids are similar, three differences were observed. The first one lies in the higher absolute value of the maximum damping force and the second in the higher increase rate of the damping force, both in the damper filled with MRF-336AG. The third one consists in higher dynamic range of the damper using MRF-132LD than that using the MRF-336AG, and this refers mostly to the greater velocity range. As for example, by kinematic excitation at frequency of 4 Hz, if the applied current was varied from 0.0 A to 0.1 A, the increase of the damping force generated by the damper using the MRF-132LD was 328 N in relation to 229 N for the damper filled with the MRF-336AG. Similarly, if the current was varied from 0.1 A to 0.2 A, the increase of the damping force was 264 N and 214 N, respectively. These results allow us to state that the MRF-132LD seems to be more suitable, in terms of control features, to the developed experimental MRF damper. For that reason some further results are presented only for the damper filled with the MRF-132LD.

a) b)

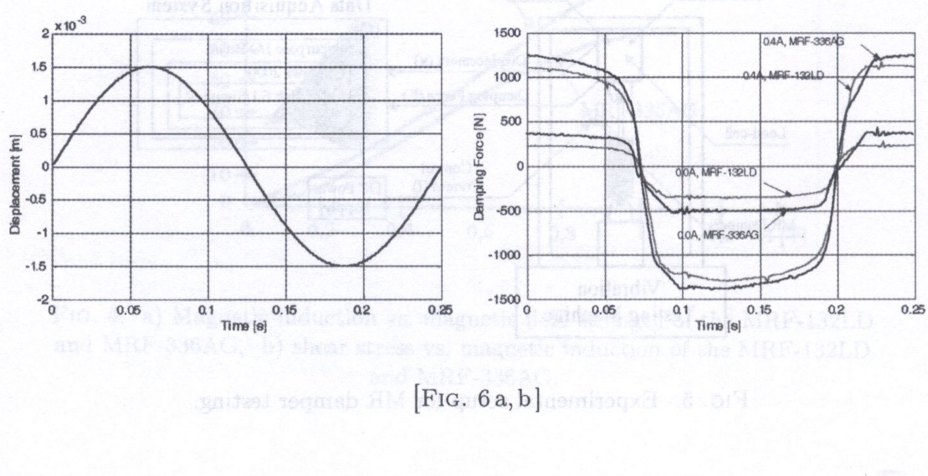

[FIG. 6 a, b]

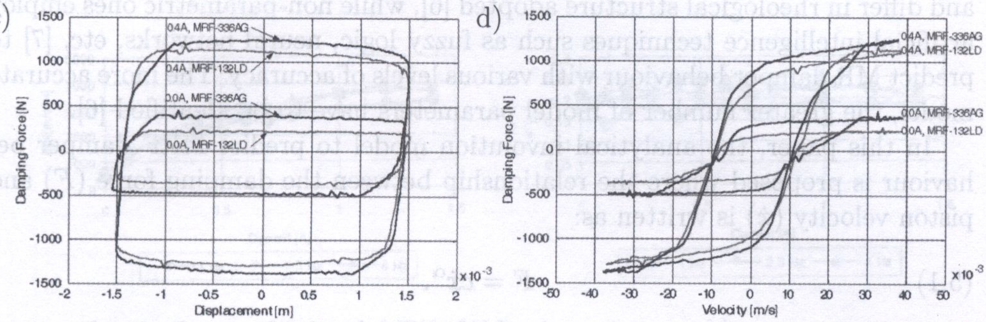

FIG. 6. Measured characteristics of the damper filled with MRF-132LD and MRF-336AG, current range (0.0, 1.4) A: a) kinematic excitation vs. time, b) damping force vs. time, c) force-displacement curve, d) force-velocity curve.

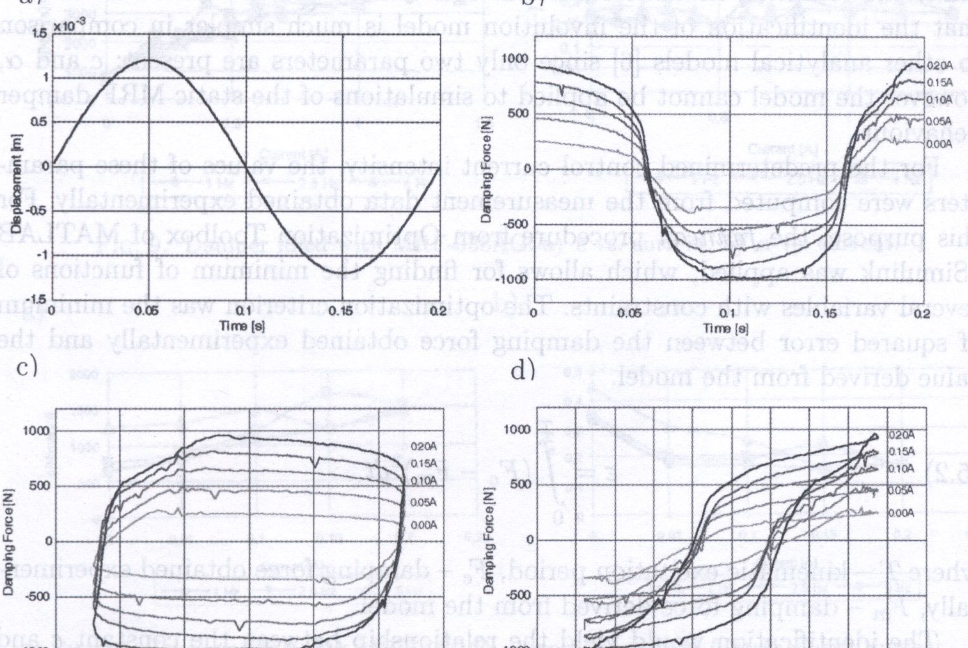

FIG. 7. Measured characteristics of the MRF damper filled with MRF-132LD, current range (0.0, 0.2) A: a) kinematic excitation vs. time, b) damping force vs. time, c) force-displacement curve, d) force-velocity curve.

5. FORMULATION OF THE INVOLUTION MODEL

Two categories of MRF dampers models, parametric and non-parametric, are available in literature. Parametric models are based on an analytical approach and differ in rheological structure adopted [6], while non-parametric ones employ artificial intelligence techniques such as fuzzy logic, neural networks, etc. [7] to predict MR damper behaviour with various levels of accuracy. The more accurate model, the greater number of model parameters have to be identified [6].

In this paper, the analytical involution model to predict MRF damper behaviour is proposed where the relationship between the damping force (F) and piston velocity ($\dot{x}$) is written as:

$$F = c\dot{x}^{\alpha}. \tag{5.1}$$

where c – a constant independent of frequency, α – power exponent (meeting the condition that $0.0 < \alpha \leq 1.0$) r. The involution model (often used to predict the behaviour of viscous fluid dampers) can be applied in case of the MRF damper because the magnitude of the damping force remains within the specified bound under the condition that the coefficient α is close to zero. It should be noticed that the identification of the involution model is much simpler in comparison to other analytical models [6] since only two parameters are present: c and α, however the model cannot be applied to simulations of the static MRF damper behaviour.

For the predetermined control current intensity, the values of these parameters were computed from the measurement data obtained experimentally. For this purpose, the *fmincon* procedure from Optimization Toolbox of MATLAB /Simulink was applied, which allows for finding the minimum of functions of several variables with constraints. The optimization criterion was the minimum of squared error between the damping force obtained experimentally and the value derived from the model.

$$\varepsilon = \int_0^T (F_e - F_m)^2 dt, \tag{5.2}$$

where T – kinematic excitation period, F_e – damping force obtained experimentally, F_m – damping force derived from the model.

The identification would yield the relationship between the constant c and the power exponent α and current intensity over the range (0.0–1.4) A, for the kinematic excitation frequency 1, 2.5, 4 Hz, (Fig. 8 – MRF damper with the fluid 132LD; Fig. 9 – MRF damper with the fluid 336AG). Parameters of the involution model of the MRF damper with the fluid 132LD were also identified for the current levels (0.0, 0.2) A. The results are provided in Fig. 10.

Besides these curves, values of involution model parameters ($F = c\dot{x}^{\alpha}$), for the damper filled with MRF-132LD and MRF-336AG (frequency 4 Hz, current range (0.0, 1.4) A), and for the damper filled with MRF-132LD (frequency 4 Hz, current range (0.0, 0.2) A), are provided in Table 2 and Table 3.

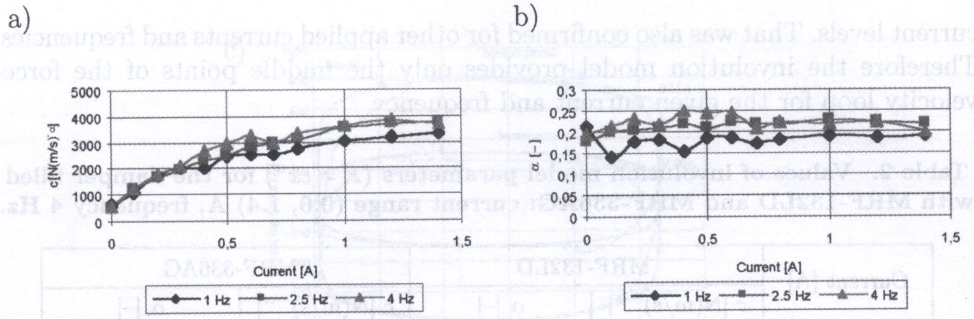

FIG. 8. Damper filled with MRF-132LD: a) c vs. current, b) α vs. current.

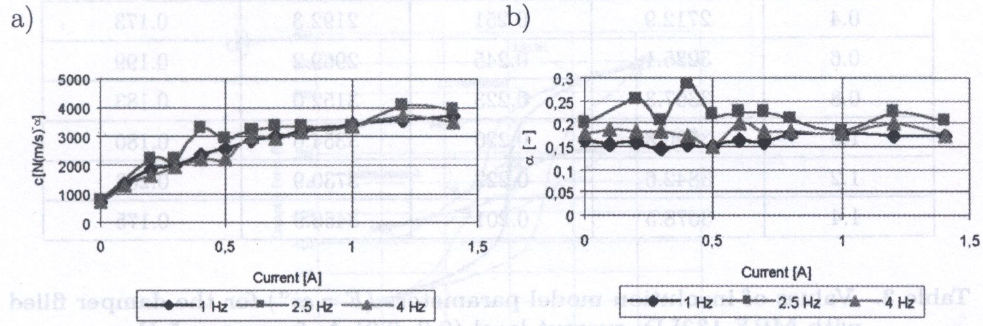

FIG. 9. Damper filled with MRF-336AG: a) c vs. current, b) α vs. current.

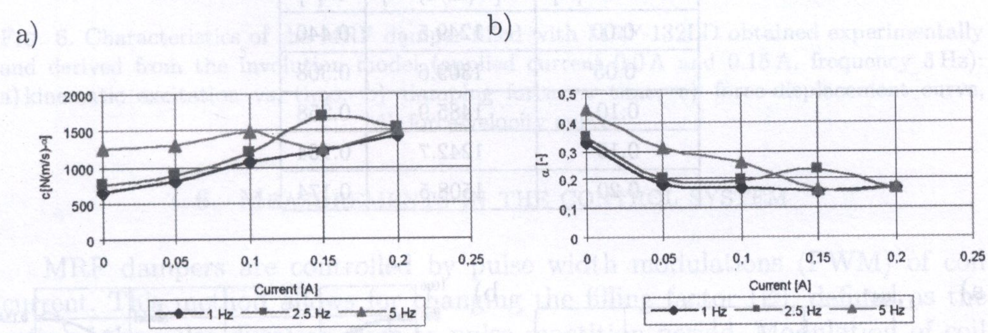

FIG. 10. Damper filled with MRF-132LD; current range (0.0, 0.2) A: a) $c$vs. current, b) α vs. current.

In Fig. 11 the experimental (measured) and derived (model) characteristics for MRF damper filled with MRF-132LD are presented. They were obtained for sine kinematic excitation (frequency 5 Hz) and for two levels of applied current 0.0 A and 0.15 A.

It is seen that the involution model does not ensure good enough fidelity to portray the actual behaviour of the damper for the applied excitation and current levels. That was also confirmed for other applied currents and frequencies. Therefore the involution model provides only the middle points of the force-velocity loop for the given current and frequency.

Table 2. Values of involution model parameters ($F = c\dot{x}^{\alpha}$) for the damper filled with MRF-132LD and MRF-336AG: current range (0.0, 1.4) A, frequency 4 Hz.

Current [A]	MRF-132LD		MRF-336AG	
	c [N(m/s)$^{-\alpha}$]	α [–]	c [N(m/s)$^{-\alpha}$]	α [–]
0.0	560.5	0.197	747.9	0.176
0.2	1811.7	0.231	1643.8	0.184
0.4	2712.9	0.251	2192.3	0.173
0.6	3235.1	0.245	2969.2	0.199
0.8	3367.3	0.223	3152.0	0.183
1.0	3596.3	0.220	3354.6	0.180
1.2	3842.6	0.222	3730.9	0.203
1.4	3678.5	0.201	3466.9	0.175

Table 3. Values of involution model parameters ($F = c\dot{x}^{\alpha}$) for the damper filled with MRF-132LD: current level (0.0, 0.2) A, frequency 5 Hz.

Current [A]	c [N(m/s)$^{-\alpha}$]	α [–]
0.00	1249.5	0.440
0.05	1309.6	0.308
0.10	1485.9	0.258
0.15	1242.7	0.164
0.20	1508.5	0.174

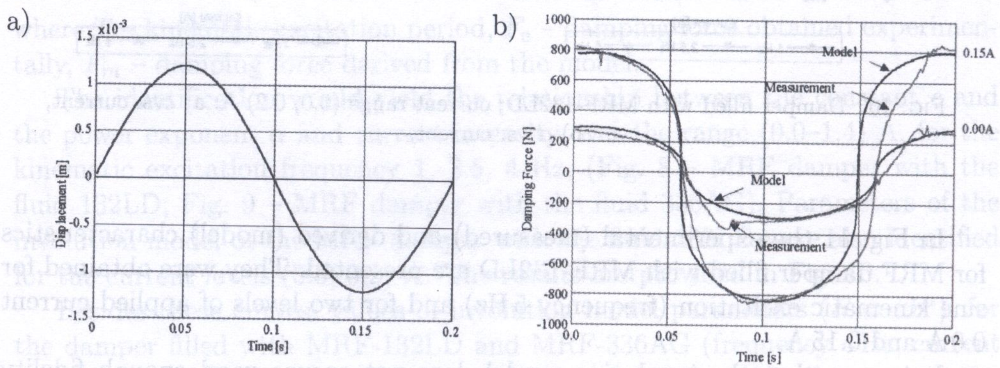

[FIG. 11 a, b]

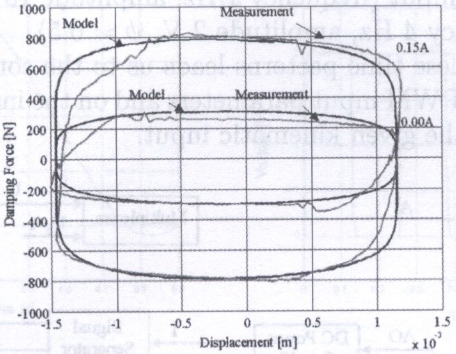

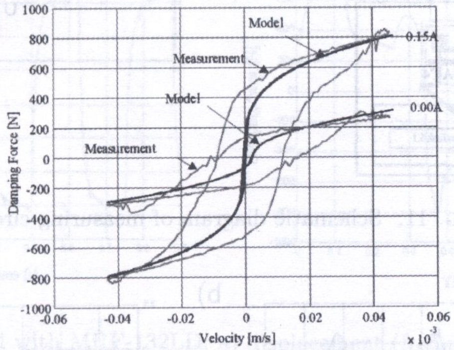

FIG. 6. Characteristics of the MRF damper filled with MRF-132LD obtained experimentally and derived from the involution model (applied current 0.0 A and 0.15 A, frequency 5 Hz): a) kinematic excitation vs. time, b) damping force vs. time, c) force-displacement curve, d) force-velocity curve.

6. Measurements in the control system

MRF dampers are controlled by pulse width modulations (PWM) of coil current. This method allows for changing the filling factor (ψ), defined as the ratio of the pulse duration time to pulse repetition period. Modulation of coil current results in variation of magnetic induction in the gap. As a result, viscosity of fluid in the gap changes and so does the damping force.

Measurements in the damper control system were taken by means of a measuring circuit shown schematically in Fig. 12.

Selected results obtained for the damper filled with MRF-132LD are shown in Fig. 13 and Fig. 14. Figure 13 presents the time patterns of kinematic input (displacement) for frequency 4 Hz, amplitude 1×10^{-3} m PWM voltage input on coil clamps (frequency 4 Hz, amplitude 2 V, variable filling rate $\psi = 0.8$ and $\psi = 0.2$) of the coil current, as well as current response to these inputs and damping force. Figure 14 presents time patterns of current and damping force for the displacement input (frequency 1 Hz, amplitude 10×10^{-3} m) and voltage input PWM (frequency 4 Hz, amplitude 2 V, $\psi = 0.5$).

The analysis of these time patterns leads us to the conclusion that damping force depends on the PWM input parameters and on the instant when the control signal is applied for the given kinematic input.

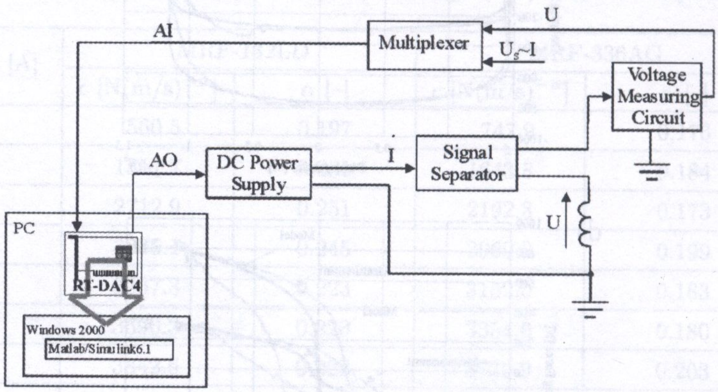

FIG. 11. Schematic diagram of measuring circuit.

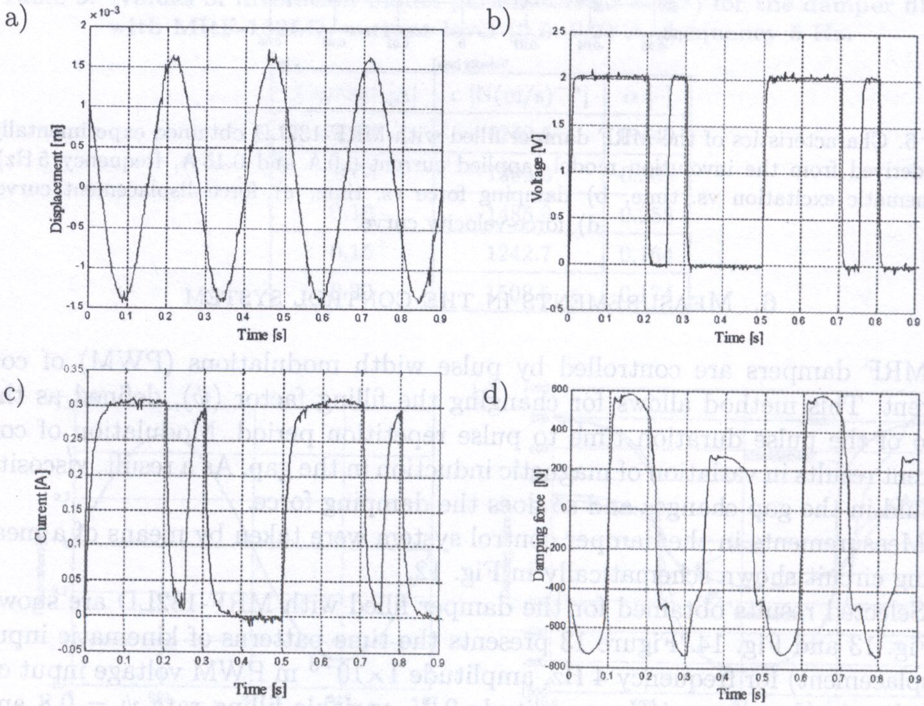

FIG. 12. Damper filled with MRF-132LD: a) displacement (frequency 4 Hz, amplitude 1.5×10^{-3} m), b) voltage (amplitude 2 V, $\psi = 0.8$, $\psi = 0.2$), c) current, d) damping force.

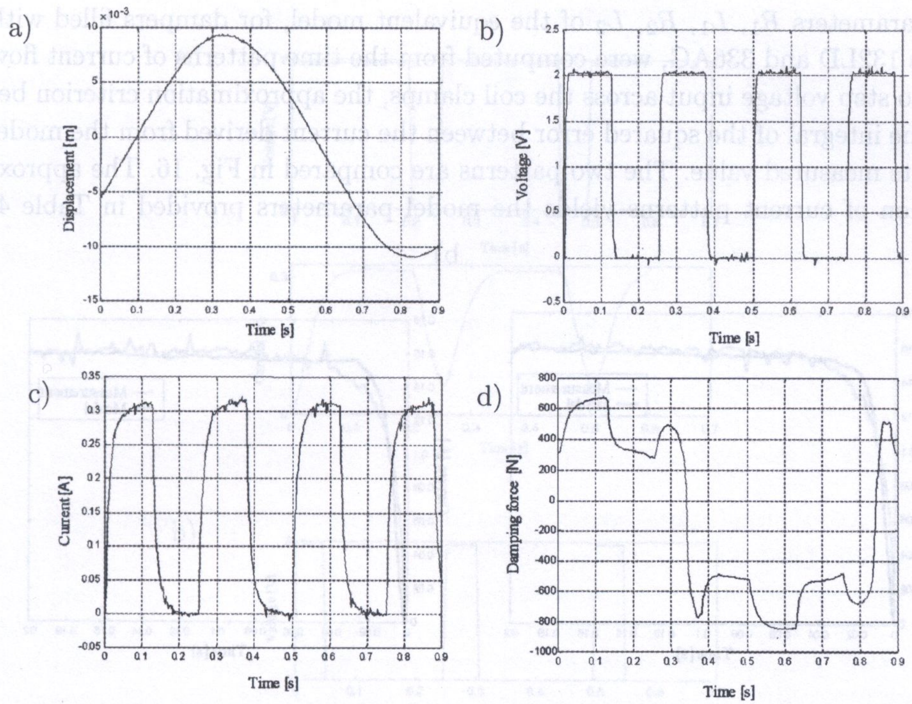

FIG. 13. Damper filled with MRF-132LD: a) displacement (frequency 1 Hz, amplitude 10×10^{-3} m), b) voltage (amplitude 2 V, $\psi = 0.5$), c) current, d) damping force.

7. FORMULATION OF THE EQUIVALENT MODEL OF THE CONTROL SYSTEM

As it was already mentioned in the introduction, the main design objectives are that over the effective current range, the steel components of the designed damper and the applied MR fluids fall in the linear section of the magnetisation characteristics. Thus, the energy processes (involving electricity) in the damper control system can be vastly simplified. It was shown in [8] that these processes determine the circuit model of the MRF damper in the form of the second order linear circuit wherein the effects of rotary currents are taken into account, (Fig. 15).

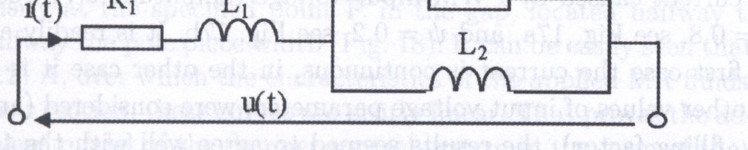

FIG. 14. Equivalent model of the control system.

Parameters R_1, L_1, R_2, L_2 of the equivalent model, for dampers filled with fluids 132LD and 336AG, were computed from the time patterns of current flow due to step voltage input across the coil clamps, the approximation criterion being the integral of the squared error between the current derived from the model and its measured value. The two patterns are compared in Fig. 16. The approximation of current patterns yields the model parameters provided in Table 4.

a) b)

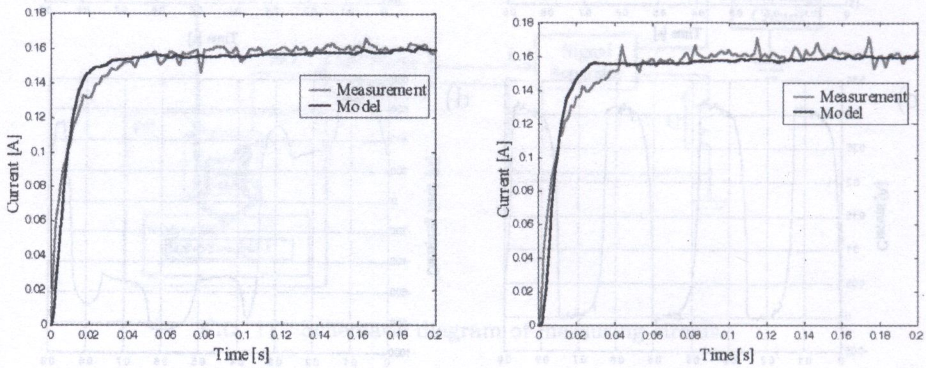

FIG. 15. Coil current flow due to step input voltage; (amplitude 1 V): a) damper filled with fluid MRF-132LD, b) damper filled with fluid MRF-336AG.

Table 4. Parameters of the equivalent model of the driving system of a damper filled with fluid.

Damper filled with MRF-132LD	Damper filled with MRF-336AG
$R_1 = 5.922$ [Ω]	$R_1 = 5.745$ [Ω]
$L_1 = 0.035$ [H]	$L_1 = 0.032$ [H]
$R_2 = 0.671$ [Ω]	$R_2 = 0.729$ [Ω]
$L_2 = 0.397$ [H]	$L_2 = 0.419$ [H]

The equivalent model presented here was then utilised to obtain the patterns of coil current caused by PWM input voltage (amplitude 2 V, frequency 4 Hz) for $\psi = 0.8$, see Fig. 17a, and $\psi = 0.2$, see Fig. 17b. It is readily apparent that in the first case the current is continuous, in the other case it is intermittent. When other values of input voltage parameters were considered (amplitude, frequency, filling factor), the results seemed to agree well with the test model [8] and measured values.

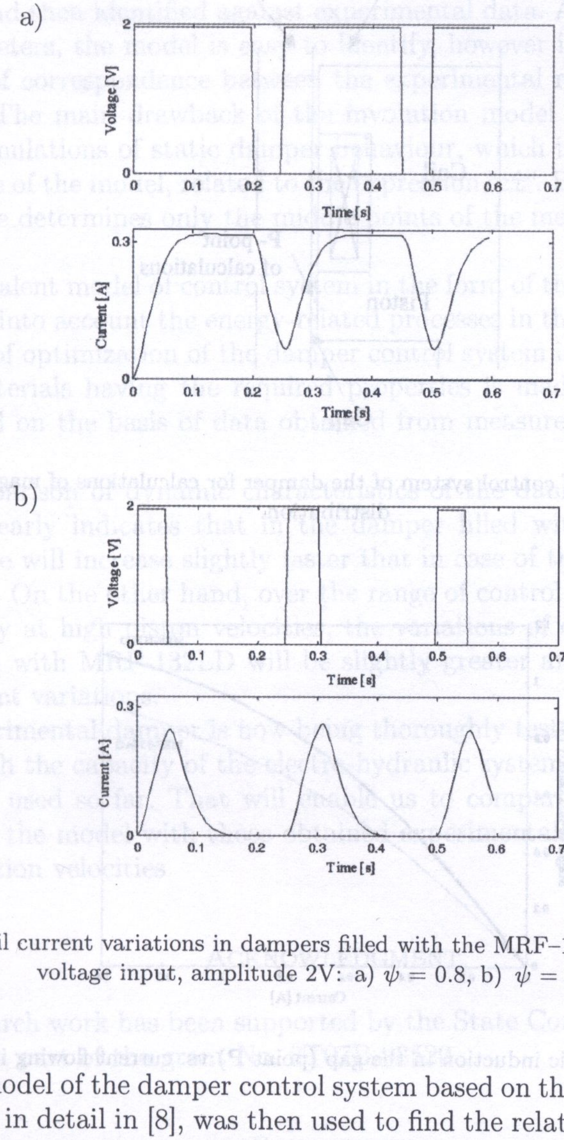

FIG. 16. Coil current variations in dampers filled with the MRF–132LD due to PWM voltage input, amplitude 2V: a) $\psi = 0.8$, b) $\psi = 0.2$.

The test model of the damper control system based on the Maxwell equations and described in detail in [8], was then used to find the relationship between the magnetic induction in the gap and intensity of the coil current. Calculations done by means of the finite element method (FEM) would yield the curves presented in Fig. 19, which represent the relationship between magnetic flux density and current intensity at the specified point **P** in the gap, located halfway the gap width and halfway the pole piece width (Fig. 18). It can be easily seen that in the range (0.0, 0.2) A, over which the characteristics of the applied MR fluids would fall in the linear section, these curves are nearly linear. That proves the adequacy of the equivalent model of the damper control system in the form of the second order linear model and coil current patterns obtained on that basis, (Fig. 17).

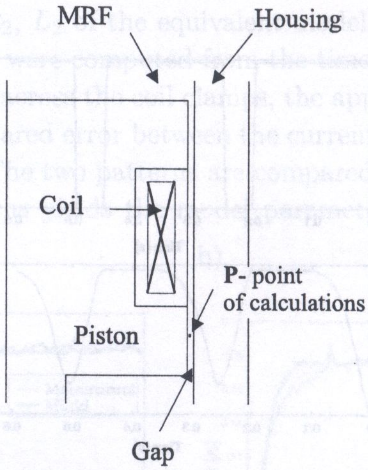

FIG. 17. Model of control system of the damper for calculations of magnetic field distribution.

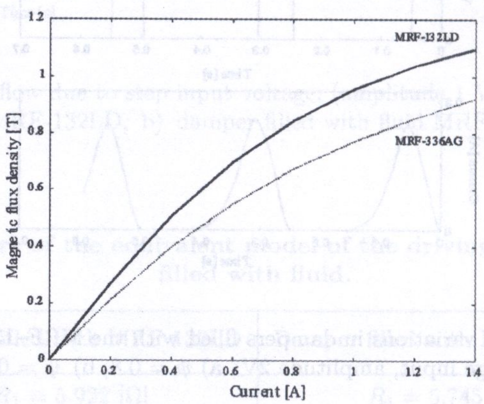

FIG. 18. Magnetic induction in the gap (point **P**) vs. current flowing in the coil.

8. Conclusions

The subject matter of the present study is investigation of dynamic characteristics of an experimental linear MRF damper filled with two types of MR fluids. Experiments on testing machines were run to find the relationship between the damping force and the piston motion rate for different levels of current.

The damping force, the force-displacement curves and the force-velocity curves were evaluated. The magnitude of the damping force depends on the input magnetic field, but it has an upper limit.

The involution model of the damper (representing force-velocity loop) was formulated and then identified against experimental data. As there are only two model parameters, the model is easy to identify, however it does not provide a high degree of correspondence between the experimental results and computer simulations. The main drawback of the involution model is that it cannot be applied to simulations of static damper behaviour, which is the result of an intrinsic feature of the model, related to the expression "$c\dot{x}$". Besides, the predicted damping force determines only the middle points of the measured force-velocity curve.

The equivalent model of control system in the form of the second order linear system takes into account the energy-related processes in the damper. Moreover, the problem of optimization of the damper control system is simplified while the choice of materials having the required properties is made easier. The model was identified on the basis of data obtained from measurements in the control circuit.

The comparison of dynamic characteristics of the damper for two types of MR fluids clearly indicates that in the damper filled with MRF-336AG, the damping force will increase slightly faster that in case of the damper filled with MRF-132LD. On the other hand, over the range of control currents (0.0, 0.2) A and especially at high piston velocities, the variations of damping force in the damper filled with MRF-132LD will be slightly greater and will correspond to control current variations.

The experimental damper is now being thoroughly tested on the testing machine in which the capacity of the electro-hydraulic system is much greater that in the tester used so far. That will enable us to compare the damping forces derived from the model with those obtained experimentally over a wider range of piston motion velocities.

Acknowledgment

The research work has been supported by the State Committee for Scientific Research as a part of the grant No. 8T07B 03520

References

1. Agrawal, P. Kulkarni, S. L. Vieira, N., G. Naganathan, *An overview of magneto- and electro-rheological fluids and their applications in fluid power systems,* **2**, 5–36, 2001.

2. R. Bolter, H. Janocha, *Design rules for MR actuators in different working modes,* SPIE, **3045**, 148–159.

3. S. B. Choi, B. K. Lee, M. H. Nam, C. C. Cheong, *Vibration control of a MR seat damper for commercial vehicle,* Smart Structures and Integrated Systems, Norman Werely, Editor, Proceedings of SPIE, **398**, 5, 2000.

4. J. E. Lindler, G. A. Dimock, N. M. Werely, *Design of a magnetorheological automotive shock absorber*, Smart Structures and Materials 2000, Smart Structures and Integrated Systems, Proceedings of SPIE, **398**, 5, 2000.

5. A. Ławniczak, A. Milecki, *Electro-rheological and magneto-rheological fluids and their application in technology* [in Polish], Wydawnictwo Politechniki Poznańskiej, 1999.

6. B. Sapiński, J. Filuś, *Analysis of parametric models of MR linear*, Journal of Theoretical and Applied Mechanics, **41**, 2, 215–240, 2003.

7. B. Sapiński, *Non-parametric representations of MR linear damper behavior*, Proceedings of the IUTAM Symposium on Dynamics of Advanced Materials and Smart Structures, Yonezawa, Japan, Kluwer Academic Publishers, 347–357, 2002.

8. B. Sapiński, *Magnetic field analysis in a magneto-rheological damper* [in Polish], Sci. Papers of the AGH University of Science and Technology, Kraków (to be published).

9. B. Sapiński, Z. Szydło, *Construction and experimental investigations of a vibration damper with magneto-rheological fluid* [in Polish], Problems of Machine Exploitation, **1**, 133, 95–106, 2003.

10. B. Sapiński, Z. Szydło, *Dash-pot damper of linear vibrations with a magneto-rheological fluid* [in Polish], Invention Project Application, P–356512, 2002.

11. G. Y. Zhou, P. Q. Zhang, *Investigation of the dynamic mechanical behavior of the doubled-barreled configuration in a magnetorheological fluid damper*, Smart Materials and Structures, **11**, 230–239, 2002.

12. United States Patents, 5, 277, 281, *Magnetorheological fluid dampers*, 1999.

13. *Real-time windows target user's guide*, The Math Works Inc., Natick, Massachusetts, 1999.

Received February 17, 2003; revised version July 28, 2003.